Journal of Applied Informatics and Computing (JAIC)
Vol.10, No.1, February 2026, pp. 468~478
e-ISSN: 2548-6861

A SEIR Metapopulation Model for Mpox Transmission Dynamics in the DRC

Kasende Mundeke Peter[1]*, Matondo Mananga Herman[2]*, Milolo Kanumuambidi Lea Irène[3]*, Pokuaa Gambrah Patience [4]**
* Department of Mathematics, Statistics and Computer Sciences, University of Kinshasa D.R. Congo
**Department of Mathematical Sciences, Faculty of Applied Sciences, Kumasi Technical University, Ghana
peter.kasende@unikin.ac.cd [1], herman.matondo@unikin.ac.cd [2], leah.milolo@unikin.ac.cd [3], patiencegambrah@yahoo.fr [4]

Article Info

Article history:

Received 2025-10-31
Revised 2025-12-13
Accepted 2025-12-22

Keyword:

Mpox,
SEIR Metapopulation,
Stability Analysis,
Basic Reproduction Number,
Sensitivity Analysis.

ABSTRACT

Understanding the mechanisms of infectious disease spread is a fundamental prerequisite for any control, management, or eradication strategy. This understanding relies on the rigorous integration of biological knowledge, mathematical tools, and computational resources, which enable in-depth analysis, the formulation of approximate numerical solutions, and the simulation of the temporal evolution of the pathological phenomenon. In this study, we develop an SEIR-type compartmental model to represent the transmission dynamics of Mpox, taking into account a metapopulation structure between two interconnected geographical areas, designated as patches 1 and 2. This model allows us to integrate the effects of interregional mobility on the spread of infection. The SageMath environment (version 9.3) was used to simulate viral dynamics within each patch, incorporating migration flows between the two regions. The system equilibria were determined and adjusted based on available data. The analysis focused on calculating the basic reproduction number, studying the stability of equilibria, and evaluating parameter sensitivity. The results suggest a gradual extinction of the disease in both patches, under certain conditions relating to mobility and recovery rates. Finally, this investigation highlights the relevance of SageMath software as a powerful tool for exploring and simulating spatially structured epidemiological models, with the ability to adapt to a variety of contexts and pathologies.

I. INTRODUCTION

Since the beginning of the 20th century, compartmental modeling has established itself as an essential tool for studying infectious diseases. Introduced by Ross's seminal work on malaria, then developed by Hammer and formalized by Kermack and McKendrick[1], [2] through the SIR model, this approach has gradually evolved towards more complex structures, such as the SEIR model, in order to better represent diseases characterized by an incubation period.

These models, translated into systems of ordinary differential equations (ODEs), make it possible to analyze transmission dynamics transmission, assess stability conditions, and determine critical thresholds for propagation.

Mpox, formerly known as monkeypox, is a re-emerging viral zoonosis whose history is closely linked to Central Africa, with the DRC alone reporting nearly 85% of known cases. This country has experienced several epidemics, the most significant of which occurred in the Katako-Kombe Health Zone in the Sankuru district (Kasaï Oriental province) [3] between 1996 and 1997, with 511 suspected cases reported. After the first human case of MPOX was identified in 1971 in a child in the DRC, cases of this disease were observed sporadically among people who had been in direct contact with infected animals. Most authors agree that after 30 years after the cessation of smallpox vaccination campaigns, there has been a significant resurgence of MPOX cases in several tropical regions, including the DRC, which is beginning to pose a real public health problem. This has sparked renewed

interest in the disease, which has been the subject of several research projects since the late 1990s. According to studies on recent MPOX epidemics, more than 90% of MPOX patients are under the age of 30 and have therefore not been vaccinated against smallpox because they were born after 1980.

Historically and culturally, the provinces of the DRC are rural areas with a strong dependence on hunting and agriculture. Infectious disease outbreaks have had a significant impact on local communities. Hunting practices, interactions with wildlife, and unprotected human contact may play a role in the transmission of MPOX; hunters, farmers, and rural communities are susceptible to catching and transmitting the virus. This context is essential for understanding the dynamics of the MPOX epidemic and for developing strategies adapted to the local reality. Recurrent outbreaks observed in the country, sometimes in densely populated urban areas, highlight the importance of appropriate mathematical tools to anticipate and control its spread.In this work, we consider an SEIR compartmental model, enriched with a metapopulation structure between two interconnected regions (patches 1 and 2). This framework allows us to take into account the effects of interregional mobility on transmission dynamics by simulating population exchanges that may influence the persistence or extinction of the disease.[4]

The numerical resolution of the system is performed using the free software SageMath (version 9.3), which integrates scientific libraries such as NumPy, SciPy, Seaborn, and Matplotlib. This environment provides a unified platform for symbolic and numerical calculations, facilitating the calculation of equilibrium points, the basic reproduction number R_0 ,as well as stability and sensitivity analysis of the parameters.

The results obtained highlight the conditions under which Mpox can gradually disappear in both patches, depending on mobility dynamics and recovery rates. This study thus illustrates the relevance of compartmental modeling and the effectiveness of SageMath for the analysis and simulation of multi-regional epidemiological models, with significant added value for the Congolese context.

II. MATHEMATICAL FORMULATION

Mathematical modeling of infectious diseases is a fundamental tool for understanding transmission dynamics, anticipating epidemic developments, and guiding public health policies. Among the most widely used compartmental models, the SEIR [2] (Susceptible–Exposed–Infectious–Recovered) model represents the key stages of infection, taking into account the incubation period before contagiousness. However, real-world epidemiological contexts are rarely homogeneous. Geographical disparities, differences in access to healthcare, social behaviors, and population mobility strongly influence the spread of pathogens. To better capture this heterogeneity, it is relevant to extend the classic SEIR model to a multi-patch structure, where each patch represents a distinct geographical or social area, interconnected by migratory flows.

In this study, we propose a mathematical formulation of the two-patch SEIR model, incorporating the effects of natural mortality, demographic recruitment, and inter-patch mobility. Each compartment (susceptible, exposed, infectious, recovered) is modeled separately for each patch, with specific parameters for transmission (β_i), progression (α_i), andhealing (γ_i), and migration (m_{ij}). The resulting system allows us to analyze the combined impact of local dynamics and spatial interactions on the evolution of the epidemic.[6]

This approach provides a flexible framework for calibration based on field data, simulation of intervention scenarios, and study of the stability of epidemic equilibria. It is part of a contextualized modeling approach, adapted to the health realities of territories with high structural variability, such as those observed in the Democratic Republic of Congo or in other regions with fragmented health systems. [7]

A. Epidemiological assumptions leading to the multi-patch SEIR model

Consider a population of size N in two different patches. With interaction m_{ij} between patches. And a set of people interacting in a single patch using a deterministic compartmental model (SEIR). With m_{ij}, the inter-patch movement rate matrices, and X = {S,E,I,R}. [5]

We consider a population distributed across two interconnected geographical zones (patches 1 and 2). Each individual belongs to one of the four compartments of the SEIR model: Susceptible (S), Exposed (E), Infectious (I), and Recovered (R).

In our modeling approach, animals remain localized in their respective areas. This assumption, although simplistic, is based on empirical and historical evidence: inter-patch movement of animals is considered negligible, in accordance with observations reported by Ejercito and Urbino, as well as Russell and Santiago. Let us further assume that the time it takes for humans to travel is very small compared to the incubation period and demographics, so that humans do not change their epidemiological status during travel and the duration of the latency period: approximately 5 to 21 days before the onset of symptoms.

1. Spatial heterogeneity of contacts

Individuals are not evenly distributed: transmission rates β_i vary across areas (patches) due to density, social behaviors, or access to healthcare. For i= 1,2

2. Inter-patch mobility

Movement between geographical areas influences propagation: migration rates m_{ij} model this

mobility.Migration flows can be asymmetrical (e.g., rural[9] exodus or seasonal movements).

3. Differentiated progression of infection

The rate of transition from exposed to infectious (α_i) depends on local factors: nutrition, comorbidities, detection times

4. Constant or seasonal recruitment

Λ_i recruitment can represent births or arrivals in the population (e.g., return of migrants). It is often assumed to be constant for simplicity, but can be modulated.

5. Natural mortality independent of disease

rate d is introduced for reflect the dynamics System of differential equations demographic system outside of an epidemic (aging, accidents,etc.). This makes it possible to better isolate the impact of the disease on the population [10] [11]

6. Local recovery dependent on the healthcare System

The recovery rate varies depending on access to care, γ_i availability of treatments, and the responsiveness of local authorities

7. No immediate reinfection

Recovered individuals move into R_i and do not immediately return to S_i , which is consistent with diseases with temporary or lasting immunity.

8. Incidence function

The transmission of infection in each patch i is modeled by a bilinear incidence function of the form

$$F_i\ (S_i, I_i) = \frac{\beta_i I_i}{N} \qquad \text{Pour i= 1,2}$$

The overall dynamics of the epidemiological model are therefore given by the following system of differentialequations

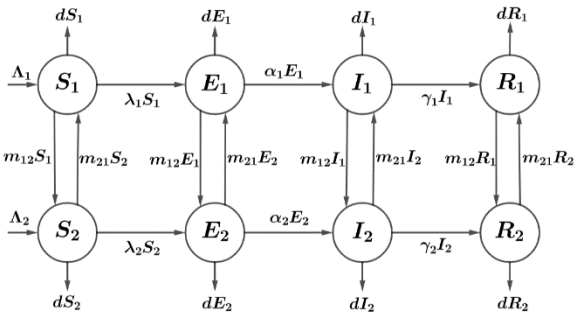

Figure 1 Mpox diagram

Compartment
S_i(t) : susceptible individuals in patch i
E_i(t) : exposed individuals (infected but not yet infectious) in patch i
I_i(t): infectious individuals in patch i
R_i(t) : recovered individuals in patch i

System of differential equations

$$\begin{aligned}
\frac{dS_i}{dt} &= \Lambda_i - \beta_i S_i I_i - dS_i - m_{ij} S_i + m_{ji} S_i \\
\frac{dE_i}{dt} &= \beta_i S_i I_i - \alpha_i E_i - dE_i - m_{ij} E_i + m_{ji} E_i \\
\frac{dI_i}{dt} &= \alpha_i E_i - \gamma_i I_i - dI_i - m_{ij} I_i + m_{ji} I_i \\
\frac{dR_i}{dt} &= \gamma_i I_i - dR_i - m_{ij} R_i + m_{ji} R_i
\end{aligned} \tag{1}$$

System (1) is solved under the following initial conditions :

$$(S_i\ (0),\ E_i\ (0),\ I_i\ (0),\ R_i\ (0)) \geq 0 \qquad (2)$$

For i= 1,2

TABLE I
TABLE DESCRIBING THE VARIABLES

Par.	Description
$\boldsymbol{\beta_1}$	Transmission rate in patch 1
$\boldsymbol{\beta_2}$	Transmission rate in patch 2
α_1	Rate of progression from exposed to infectious state in patch 1
α_2	Rate of progression from exposed to infectious state in patch 2
γ_1	Recovery rate in patch 1
γ_2	Recovery rate in patch 2
d	Natural mortality rate
$\boldsymbol{\Lambda_1}$	Recruitment rate (births or immigration in each patch 1)
$\boldsymbol{\Lambda_2}$	Recruitment rate (births or immigration in each patch 2)
m_{12}	Migration rate from patch 1 to patch 2
m_{21}	Migration rate from patch 2 to patch 1

Notes 1.

The terms m_{ij} model mobility between the two patches. Recruitmen Λ_i is assumed to be constant and identical in the two patches, but it can be adapted $\Lambda_1\ and\ \Lambda_2$ if necessary. The system is coupled by migration terms, which allows us to study the impact of mobility on the dynamics ofthe epidemic.

III. MATERIALS AND METHODS

The SEIR model considered in this study is formalized by a system of ordinary differential equations (ODEs), as shown in equation (1) and illustrated in Figure 1. The model diagram was generated using GeoGebra software (version 6.0.848.0) on a machine equipped with a 1.10 GHz Intel Celeron N4020 processor, 6 GB of RAM, a 932 GB SSD (LS 1TB M300), and an Intel UHD Graphics 600 (128 MB) graphics card, running on a 64-bit operating system.

All numerical analyses were performed using SageMath (version 9.3). This software allowed us to :

- Calculation of the system's equilibrium points;
- Estimating the basic reproduction number (R_0) ;
- Simulation of equilibrium stability;
- Sensitivity analysis of parameters influencing R_0.

The data used for model adjustment and validation were obtained from the Ministry of Public Health, Hygiene, and Social Action, the National Institute for Biomedical Research [6], complementary scientific sources.

IV. RESULTS AND DISCUSSION

A. Results

This section examines the fundamental properties of the SEIR [10] model applied to Mpox. It addresses successively :

- the positivity of the solutions,
- the boundedness of trajectories,
- invariance of the admissible domain,
- the equilibrium of the system,
- the basic reproduction number R_0,
- and the stability of equilibrium states.

1. Consider the following compact invariant domain :

$$\Omega = \{ (S_i , E_i , I_i , R_i) \in R_+^8 : 0 < N \leq \frac{\Lambda}{d+ m_{21}- m_{12}}\} \qquad (3)$$

for i= 1,2

Theorem1. The system model (1) is well established both biologically and mathematically. [12]

Proof**:** We demonstrate this theorem step by step.
Step 1:
We show that system (1) has a unique solution. The functions of system (1) are of class C^1, so they are continuous in an open ball containing the initial conditions $(S_i(0),E_i(0), I_i(0), R_i(0))$ and are locally Lipschitz, so there exists a unique local maximum solution for system (1) in Ω. for i= 1,2

Step 2 :
We show that the solutions to system (1) are positive. Starting from system (1), we have : [12]

$$\frac{dS_i}{dt} \mid (S_i = 0)(E_i, I_i R_i) > 0 \ = \Lambda_i$$

$$\frac{dE_i}{dt} \mid (E_i = 0)(S_i, I_i R_i) > 0 \ = \beta_i S_i I_i$$

$$\frac{dI_i}{dt} \mid (I_i = 0)(S_i, E_i R_i) > 0 \ = \alpha_i E_i$$

$$\frac{dR_i}{dt} \mid (R_i = 0)(S_i, E_i I_i) > 0 \ = \gamma_i I_i$$

for i= 1,2

We can conclude that all solutions of the system (1) are positive.

Step 3.
By adding the equations of system (1), we obtain

$$\begin{aligned} N &= N_1 + N_2 \\ &= S_1 + E_1 + I_1 + R_1 + S_2 + E_2 + I_2 + R_2 \\ &= \Lambda - (d + m_{21} - m_{12}) N \end{aligned}$$

Which implies

$$N(t) \leq \left(\frac{\Lambda}{d+ m_{21}- m_{12}} - \left(\frac{\Lambda}{d+ m_{21}- m_{12}} - N(0)\right)e^{(d+ m_{21}- m_{12})t} \right)$$

Using the constant variation formula, we get.

$$\lim_{t \to \infty} Sup(t) = \frac{\Lambda}{d+ m_{21}- m_{12}} \qquad (4)$$

Thus, $N(t) = \frac{\Lambda}{d+ m_{21}- m_{12}}$. This allows us to conclude that, the set of solutions $\{(S_i(t) , E_i(t), I_i(t), R_i(t)) \}$ is bounded ins Ω, i.e

$$\Omega = \{ (S_i,E_i, I_i, R_i) \in R_+^8 : 0 < N \leq \frac{\Lambda}{d+ m_{21}- m_{12}}\}$$

for i= 1,2

Therefore, all solutions of system (1) are bounded in the Region Ω which attracts all solutions in R_+^8

Given all this, we conclude that for the initial condition (S(0),E(0),$I(0)$,$R(0)$) contained in the positively invariant

Domain Ω, le système (1) admits a unique, non-negative solution.

2. Disease Free Equilibrium (DFE) and basic reproduction number (R_0)

Model (1) admits two equilibrium points, namely: the disease-free equilibrium point X^0 which appears in the absence of any infection, i.e. (E=0, I=0), and the endemic equilibrium X^* which appears in the presence of infection, i.e. ($E\neq0$, $I\neq0$). [13]

À partir de ce qui précède, l'équilibre sans maladie est donné par

$$X^0 = (S^0, E^0, I^0, R^0) = (\frac{\Lambda}{d+m_{21}-m_{12}}, 0,0,0) \quad (5)$$

and the endemic equilibrium point is given by

$$X^* = (S^*, E^*, I^*, R^*)$$

Where

$$\begin{aligned} S^* &= (\Lambda_i - \beta_i\ I_i^*) / (d + m_{21} - m_{12}) \\ E^* &= (\beta_i S_i^* I_i^*) / (d + m_{21} - m_{12}) \\ R^* &= (\gamma_i I_i^*) / (d + m_{21} - m_{12}) \end{aligned} \quad (6)$$

for i= 1,2

Note 2.

Considering the equations S^* à R^*, if I^*=0, we obtain the equilibrium without disease X^0.

3. Basic reproduction number

A crucial indicator of infectious diseases is the number basic reproduction number (R_0), defined as the average number of secondary cases that a typical infectious individual produces when introduced into a population composed entirely of susceptible individuals. It is calculated using the van den Driessche [12] algorithm. After calculation in SageMath, we obtain the new infection production matrix F and the transition matrix and the inverse of the V^{-1}. [14]

$$F = \begin{pmatrix} 0 & 0 & S_0\beta_2 & 0 \\ 0 & 0 & 0 & S_0\beta_2 \\ 0 & 0 & 0 & 0 \\ 0 & 0 & 0 & 0 \end{pmatrix}$$

$$V = \begin{pmatrix} x+y & 0 & 0 & 0 \\ 0 & x+y & 0 & 0 \\ -\alpha_1 & 0 & x+y & 0 \\ 0 & -\alpha_2 & 0 & x+y \end{pmatrix}$$

With

$$x = \alpha_1 + d_1$$
$$y = m_{12} - m_{21}$$

And

$$V^{-1} = \begin{pmatrix} \frac{1}{x+y} & 0 & 0 & 0 \\ 0 & \frac{1}{x+y} & 0 & 0 \\ \frac{\alpha_1}{(x+y)^2} & 0 & \frac{1}{x+y} & 0 \\ 0 & \frac{\alpha_2}{(x+y)^2} & 0 & \frac{1}{x+y} \end{pmatrix}$$

Thus, the basic reproduction number obtained from the pectral radius of the new generation matrix ($R_0 = FV^{-1}$) is therefore

$$R_0 = \begin{pmatrix} \frac{S_0\alpha_1\beta_2}{(x+y)^2} & 0 & \frac{S_0\beta_2}{x+y} & 0 \\ 0 & \frac{S_0\alpha_2\beta_2}{(x+y)^2} & 0 & \frac{S_0\beta_2}{x+y} \\ 0 & 0 & 0 & 0 \\ 0 & 0 & 0 & 0 \end{pmatrix}$$

If
A = $2\alpha_1 - d_1$,
B = $\alpha^2 - d_1^2$
C = $m_{12}m_{21}$

and

$k_1 = d_1^2 + m_{12}^2 - m_{21}^2$
$k_2 = m_{12} - m_{21}$
$k_3 = 4\alpha_1 + 2d_1$
$k_4 = m_{12}^2 + m_{21}^2$

Then

$$R_0 = \rho\left(\frac{\Lambda\,\alpha_2\beta_2}{\alpha_1^2 d_1+(k_1)A-(k_2)B+(k_3+3(k_2))C-k_4}, , \frac{\Lambda\,\alpha_1\beta_2}{\alpha_1^2 d_1+(k_1)A-(k_2)B+(k_3+3(k_2))C-k_4}, 0,0\right)$$

TABLE II
PARAMETERS AND THEIR VALUE

Parameter	Values	Reference
Λ_2	0.05	[3]
γ_1	0.03	[3]
α_2	0.40	[3]
β_1	0.60	[15]
β_2	0.60	[15]
α_1	0.50	[3]
γ_2	0.03	[3]
d	0.1	[16]
Λ_1	0.05	[3]
m_{12}	0.00009	[16]
m_{21}	0.00015	[16]

Thus

$$R_0 = \max\{0.352, 0.441, 0,0\}$$

$$R_0 \approx 0.44$$

Part of the basic reproduction number R_0 is represented as a function depending on the parameters α_i *and* β_2 identified as the most decisive in the evolution of R_0.

In order to illustrate the impact of these parameters on the behavior of the model, the SageMath code below can be used to generate the corresponding curves,

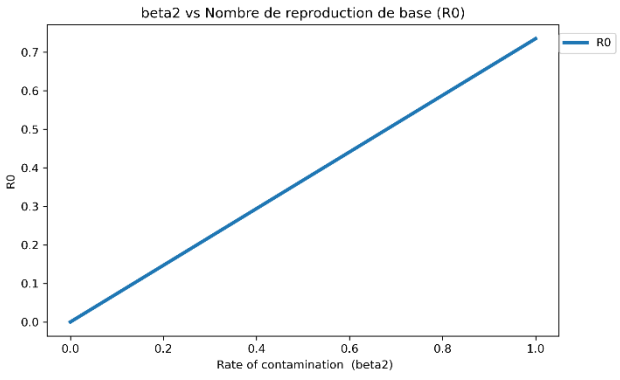

Figure 2, Evolution of the profile as a function of the value of β_2

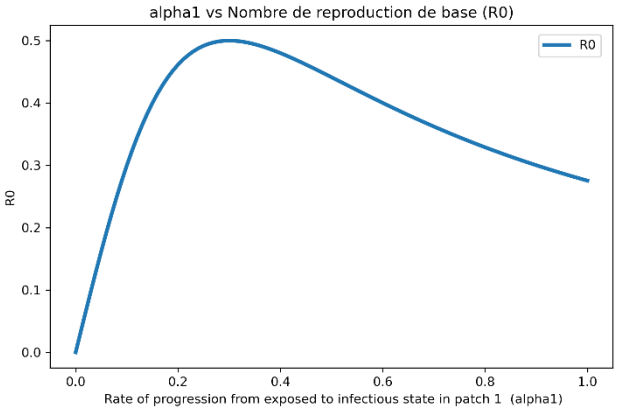

Figure 3, Evolution of the profile as a function of the value *of* α_2

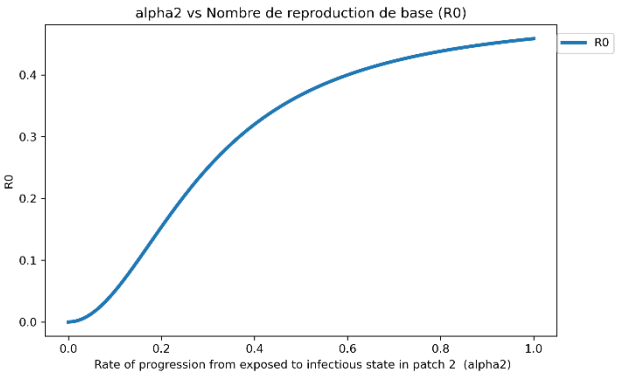

Figure 4, Evolution of the profile as a function of the value $of\ \alpha_1$

4. Global stability of the DFE

The equilibrium without disease X^0 is studied in this subsection using the method developed by. Based on this method, system (1) is rewritten as system (7) below. [17], [18]

$$\frac{dA_1}{dt} = f_1(A_1, A_2)$$
$$\frac{dA_2}{dt} = f_2(A_1, A_2), \quad f_2(A_1, 0), \tag{7}$$

Where A_1 represents the non-infectious compartments, $A_1 = (S_i, R_i) \in R_+^4$ and A_2 representthe infectious compartments, $A_2 = (E_i, I_i) \in R_+^4$ The equilibrium point without Mpox is given in this case byX^0=(A_1^0,0) and will be globally asymptotically stable (GAS) for R_0<1, if the two conditions below are satisfied:

1. for $\frac{dA_1}{dt} = f_1(A_1, 0)$ where (A_1^0,0) is and globally asymptotically stable (GAS)
2. $f_2(A_1, A_2) = GA_2 - f(A_1, A_2)$
   $Where\ f(A_1, A_2) \geq 0,$
   $For\ all\ (A_1, A_2)\ dans\ \Omega$

With $Z = DA_2(A_1^0, 0)$ is M-matrix.

Theorem 2. The disease-free equilibrium points X^0=(A_1^0,0) of model (1) are globally asymptotically stable (GAS) for R_0<1 if conditions 1 and 2 above are satisfied. [17]

Proof. Considering model

(1) $f_1(A_1, A_2)$ et $f_2(A_1, A_2)$

are defined as follows:

$$f_1(A_1, A_2) = \begin{matrix} \Lambda_1 - \beta_1 S_1 I_1 - dS_1 - m_{21} S_1 + m_{12} S_1 \\ \Lambda_2 - \beta_2 S_2 I_2 - dS_2 - m_{12} S_2 + m_{21} S_2 \\ \gamma_1 I_1 - dR_1 - m_{21} R_1 + m_{12} R_1 \\ \gamma_2 I_2 - dR_2 - m_{12} R_2 + m_{21} R_2 \end{matrix}$$

and

$$f_2(A_1, A_2) = \begin{matrix} \beta_1 S_1 I_1 - \alpha_1 E_1 - dE_1 - m_{21} E_i + m_{12} E_i \\ \beta_2 S_2 I_2 - \alpha_2 E_2 - dE_2 - m_{12} E_2 + m_{21} E_2 \\ \alpha_1 E_1 - \gamma_1 I_1 - dI_1 - m_{21} I_1 + m_{12} I_{12} \\ \alpha_2 E_2 - \gamma_2 I_2 - dI_i - m_{12} I_2 + m_{21} I_2 \end{matrix}$$

From the above, we can easily show that

$f_2(A_1, 0) = 0$

and

$$f_1(A_1, 0) = \begin{matrix} \Lambda_1 - dS_1 - m_{21} S_1 + m_{12} S_1 \\ \Lambda_2 - dS_2 - m_{12} S_2 + m_{21} S_2 \\ -dR_1 - m_{21} R_1 + m_{12} R_1 \\ -dR_2 - m_{12} R_2 + m_{21} R_2 \end{matrix}$$

Regarding condition 1, we have

$$\frac{dA_1}{dt} = f_1(A_1, 0) = \begin{matrix} \Lambda_1 - dS_1 - m_{21} S_1 + m_{12} S_1 \\ \Lambda_2 - dS_2 - m_{12} S_2 + m_{21} S_2 \\ -dR_1 - m_{21} R_1 + m_{12} R_1 \\ -dR_2 - m_{12} R_2 + m_{21} R_2 \end{matrix}$$

By analytically solving system (8), and tending towards $t \to +\infty$, we obtain

$$S_i(t) = \left(\frac{\Lambda_i}{d + m_{21} - m_{12}}\right) \text{ and } R_i(t) = 0$$

Where $X^0 = \left(\frac{\Lambda_i}{d + m_{21} - m_{12}}, 0,0,0\right)$ is GAS for

$$\frac{dA_1}{dt} = f_1(A_1, 0).$$

This satisfies the first condition 1. Now the second condition 2 is also satisfied. Looking at the system (1), the matrices G and $f(A_1, A_2)$ can be written as

$$G = \begin{pmatrix} -x + y & 0 & \beta S^0 & 0 \\ 0 & -xE_2 + y & 0 & \beta S^0 \\ \alpha_1 & 0 & -\gamma_1 - d_1 + y & 0 \\ 0 & \alpha_2 & 0 & x + y \end{pmatrix}$$

and

$$f(A_1, A_2) = \begin{pmatrix} \beta_1 (1 - \frac{S_1}{N}) I_1 \\ \beta_2 (1 - \frac{S_2}{N}) I_2 \\ 0 \\ 0 \end{pmatrix}$$

Since $0 \le S \le N$, $(1 - \frac{S}{N}) \ge 0$, it is clear that G $\ge$ 0. We *N* also note that the matrix G is an M-matrix(all non-diagonal elements of G are non-negative). Since condition 2 is satisfied, this proves that X^0 is globally asymptotically stable (GAS) for $R_0 < 1$.

5. Global stability of Endemic Equilibrium

Theorem 3. The endemic equilibrium X^* of model (1) is globally asymptotically stable (GAS) when R_0 >1. [19]

Preuve. Proof. Consider the differentiable function with value positive following :

$$L = 1/2 \left[(S - S_1^*) + (E - E_1^*) + (I - I_1^*) + (R - R_1^*) \right]^2 \quad (9)$$

The time derivative of L gives us

$$\frac{dL}{dt} = [\,(\mathcal{S} - S^*) + (E - E^*) + (I - I^*) + (R - R^*)\,]\,\frac{d}{dt}(S_1 + E_1 + I_1 + R_1)$$

$$= [(S_1 + E_1 + I_1 + R_1) + (S_1^* + E_1^* + I_1^* + R_1^*)]\frac{d}{dt}(S_1 + E_1 + I_1 + R_1)$$

$$= [(S_1 + E_1 + I_1 + R_1) + (S_1^* + E_1^* + I_1^* + R_1^*)]\,[(\Lambda_i) - (d + m_{21} - m_{12})(S_1 + E_1 + I_1 + R_1)]$$

$$= [(S_1 + E_1 + I_1 + R_1) - (S_1^* + E_1^* + I_1^* + R_1^*)]\,[-(S_1 + E_1 + I_1 + R_1)(d + m_{21} - m_{12}) + (S_1^* + E_1^* + I_1^* + R_1^*)(d + m_{12} - m_{21})]$$

Let's set $(d + m_{21} - m_{12}) = (d + m_{12} - m_{21})$,

we have:

$$= [(S_1 + E_1 + I_1 + R_1) - (S_1^* + E_1^* + I_1^* + R_1^*)]\,[-(S_1 + E_1 + I_1 + R_1) + (S_1^* + E_1^* + I_1^* + R_1^*)]\,(d + m_{21} - m_{12})$$

$$= -(d + m_{21} - m_{12})\,[(S_1 + E_1 + I_1 + R_1) - (S_1^* + E_1^* + I_1^* + R_1^*)]^2$$

Clearly, dL/dt is defined as negative.

We can therefore conclude that the function chosen above is indeed a Lyapunov function.

dL/dt=0 if and only if $S=S^*$, $E=E^*$, $I=I^*$.

It follows, according to LaSalle's invariance principle, that the largest invariant set in Ω is the singleton $\{X^*\}$. This implies that the endemic equilibrium is GAS.

6. Sensitivity analysis

We will analyze the stability using the approach of Typically, in an epidemiological context, the definition of the basic reproduction number (R_0) refers to the epidemiological threshold including the value 1, where, if R_0>1, an epidemic may occur, and if R_0<1, the disease cannot establish it self, and an epidemic is not expected. [20]

This analysis identifies the most influential parameters. The following formula calculates the sensitivity of all the parameters that make up R_0.

$$\frac{\partial R_0}{\partial \omega} * \frac{\omega}{R_0} \qquad (10)$$

Where ω is the parameter of R_0.

The sensitivity analysis is thus performed in SageMath and we have this results :

TABLE III
SENSITIVITY PARAMETERS

Parameter	Values using	Sensibilité Values	Interpretation
β_1	0.60	0.000	Negligible impact
β_2	0.40	**1.000**	Dominant parameter, priority control
α_1	0.50	-0.764	Marked negative effect (reduced R_0 acceleration)
α_2	0.03	-0.001	Very low impact
Λ	0.10	**1.000**	Dominant parameter, direct influence on R_0
m_{12}	0.00009	0.0004	Weak effect, asymmetrical
m_{21}	0.00015	-0.0007	Weak effect, asymmetrical

Numerical values are reported up to three decimal places.

Readability**:** Both figures and tables are integrated into the text with explanations, making them not only legible but also contextually meaningful. The captions and references in the discussion section confirm their interpretability.
In short, the visual elements meet academic standards: they are clear, precise, and support the mathematical and epidemiological analysis.

This reveals that:

The Parameters dominant:
β_2 (Transmission rate in patch 2) and Λ (recruitment) are the most sensitive. These are priority levers for controlling the epidemic. Effect of the progression: α_1 has a marked negative effect, meaning that accelerating transition from exposed to infectious state in patch 1 reduced R_0 — counterintuitive, but this may reflect a local dynamic where infected individuals are better cared for. Inter-patch mobility: the rates m_{12} and m_{21} have a weak but asymmetric effect onR_0, highlighting the importance of the direction of migration flows.

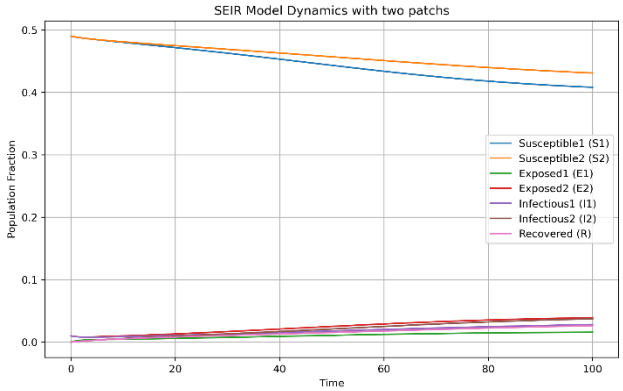

Figure 5, Evolution of mpox over time **(R_0< 1)**

When the basic reproduction number R_0 is less than 1, it means that each infected individual transmits thedisease to less than one person on average. In this context, the temporal evolution of mpox shows a gradual decline in the number of cases, reflecting a long-term trend toward the disappearance of the disease. This situation reflects the effectiveness of the control measures put in place—such as targeted vaccination, isolation of cases, and community awareness—which are successful in breaking the chains of transmission. The system then tends toward equilibrium without disease, confirming the overall stability of this state in the model.

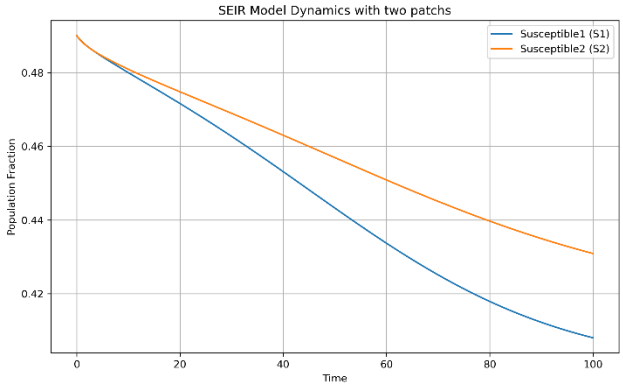

Figure 6, Evolution of susceptible individuals over time. **(R_0< 1)**

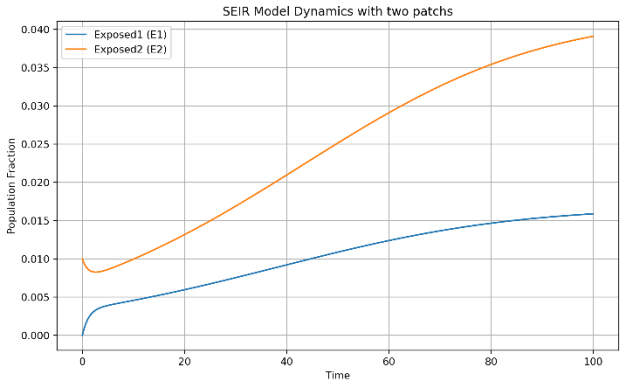

Figure 7, Evolution of exposed individuals over time.
(R_0< 1)

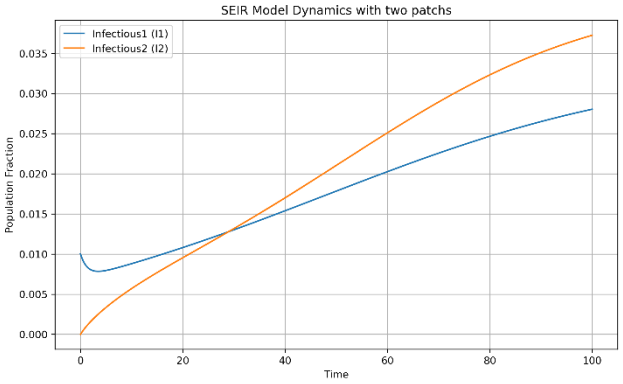

Figure 8, Evolution of infectious individuals over time.**(R_0< 1)**

Figures 6, 7, and 8: The majority of the population remains in the susceptible compartment, indicating low exposure to the disease and sustainable protection dynamics. The number of exposed individuals is rapidly decreasing, reflecting a break in the chain of transmission and slow progression toward infection. The infectious population is continuously decreasing, confirming that the disease is no longer actively spreading and is tending toward extinction**.**

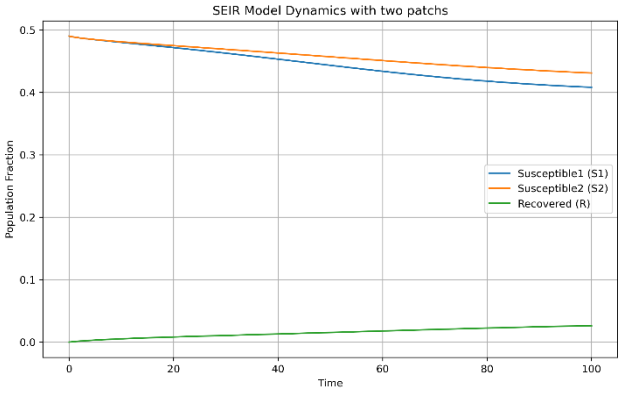

Figure 9, Evolution of susceptible individuals vs individuals recovered over time. **(R_0< 1)**

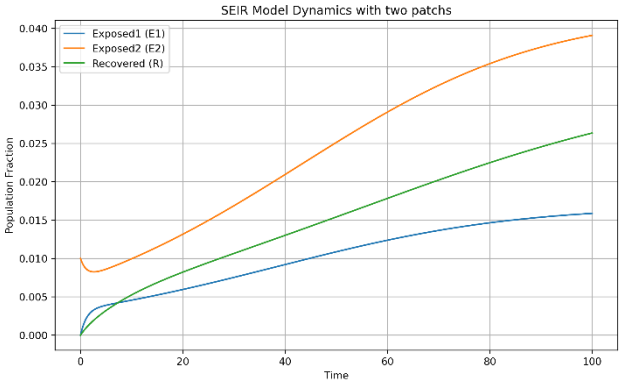

Figure 10, Evolution of exposed individuals vs individuals recovered over time. **(R_0< 1)**

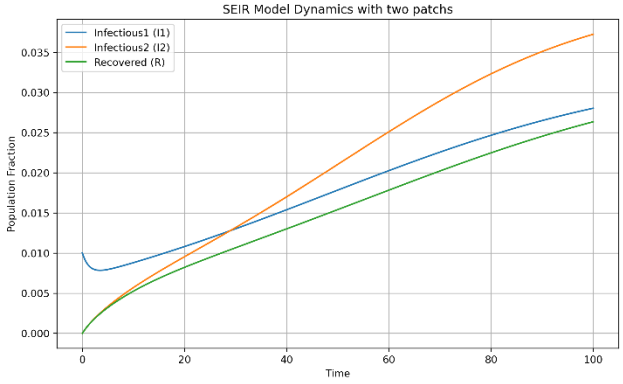

Figure 11, Evolution of infectious individuals vs individuals recovered over time. **(R_0< 1).**

B. Discussion

The use of a two-patch compartmental structure better captures the spatial heterogeneity observed in the spread of Mpox in the DRC. Unlike homogeneous models, this approach incorporates disparities in density, access to care, and social behaviors, providing a more accurate representation of local dynamics. Graphical analysis reveals epidemiological dynamics favorable to the extinction of Mpox in both patches. Figure 6 shows continued growth in the number of susceptible individuals, reflecting low exposure to infection and effective control measures. At the same time, Figures 7 and 8 show a rapid decline in exposed and infectious individuals, confirming the gradual interruption of the chain of transmission. [8]

Numerical simulations highlight a progressive decline in prevalence when the basic reproduction number R_0< 1. This result is consistent with classical epidemiological theory, confirming that disease extinction is achievable under conditions of sufficient recovery rates and controlled mobility. Graphical outputs further show that the majority of the population remains in the susceptible compartment, while exposed and infectious individuals decrease rapidly, reflecting the interruption of transmission chains.

Sensitivity analysis emphasizes the dominant influence of the transmission rate β_2 and recruitment Λ on epidemic persistence. These parameters emerge as priority levers for intervention, suggesting that surveillance and control measures should focus on regions with high transmission potential and demographic influx. Interestingly, the progression parameter α_1 exhibits a negative sensitivity, indicating that accelerating the transition from exposed to infectious states may paradoxically reduce R_0. This counterintuitive result underscores the importance of local healthcare responses, where rapid detection and management of infectious individuals can mitigate spread.

Inter-patch mobility m_{12}, m_{21} plays a secondary but asymmetric role, highlighting how directional migration flows—such as rural-to-urban movements—can subtly alter epidemic trajectories. This finding reinforces the need for coordinated surveillance across regions, particularly in areas with seasonal or economic migration patterns.

From a methodological standpoint, the model is mathematically well-posed: solutions are positive, bounded, and biologically coherent. Stability analyses using Lyapunov [21] functions and LaSalle's invariance principle confirm the robustness of both disease-free and endemic equilibria. These theoretical guarantees strengthen the legitimacy of the model as a decision-support tool for public health authorities.

Nevertheless, certain limitations must be acknowledged. The assumptions of constant recruitment and absence of immediate reinfection simplify the dynamics but may not fully reflect real-world conditions. Incorporating stochasticity, age-structure, or larger multi-patch networks could enhance predictive accuracy. Moreover, calibration with finer empirical data would improve the model's applicability to specific provinces and outbreak scenarios.

In conclusion, this study demonstrates that compartmental models enriched with spatial heterogeneity can provide actionable insights for epidemic control. In the case of Mpox in the DRC, the findings advocate for interventions focused on transmission hotspots, demographic surveillance, and interregional coordination. Beyond Mpox, the proposed framework offers a versatile foundation for analyzing other zoonotic or vector-borne diseases in fragmented health systems.

V. CONCLUSION

This study formalized and analyzed a two-patch SEIR compartmental model, integrating the effects of interregional mobility on the transmission dynamics of Mpox in the Democratic Republic of Congo. The multi-patch structure proved particularly relevant for capturing the spatial heterogeneity of health, social, and demographic contexts, while offering flexibility for calibration using local data.

The results confirm the mathematical validity of the model, with positive, bounded, and biologically consistent solutions.

Stability analysis shows that the extinction or persistence of the epidemic strongly depends on the basic reproduction number R0, which is itself influenced by key parameters such as transmission and progression rates. The sensitivity of the model to these parameters highlights the importance of targeted surveillance and differentiated intervention depending on the area.

The use of SageMath as a simulation environment has proven to be effective, accessible, and reproducible, strengthening local capacity to explore complex epidemiological scenarios. This work thus paves the way for contextualized modeling capable of supporting decision-makers in designing control strategies adapted to the realities of the Congo.

Finally, beyond Mpox, the proposed framework can be extended to other vector-borne or zoonotic diseases in contexts with high geographical variability. It provides a

promising basis for the development of public health decision support tools, combining mathematical rigor, local relevance, and digital accessibility.

BIBLIOGRAPHY

[1] S. Bowong and S. Bowong, 'CAFHOMEC-BMGF 2024 Mod´elisation et analyse pour la sant´e des femmes'.

[2] S. Bowong, 'Le modèle de Kermack et McKendrick'.

[3] E. P. S. Mbelambela, A. J. P. Wandja, A. F. Villanueva, N. D. Olamba, L. Omba, and S. M. J. Muchanga, 'Clinical characteristics of suspected cases of human mpox (monkeypox) in Katako-Kombe, Democratic Republic of the Congo 2023: challenges and key responses', *Eur. J. Clin. Microbiol. Infect. Dis.*, vol. 44, no. 3, pp. 609–617, Mar. 2025, doi: 10.1007/s10096-024-05022-3.

[4] '8_Medecine_Generale_Pierre_Lea_these'.

[5] O. J. Peter, S. Kumar, N. Kumari, F. A. Oguntolu, K. Oshinubi, and R. Musa, 'Transmission dynamics of Monkeypox virus: a mathematical modelling approach', *Model. Earth Syst. Environ.*, vol. 8, no. 3, pp. 3423–3434, Sept. 2022, doi: 10.1007/s40808-021-01313-2.

[6] R. A. Ahmad *et al.*, 'Modeling social interaction and metapopulation mobility of the COVID-19 pandemic in main cities of highly populated Java Island, Indonesia: An agent-based modeling approach', *Front. Ecol. Evol.*, vol. 10, p. 958651, Jan. 2023, doi: 10.3389/fevo.2022.958651.

[7] 'Modélisation-mathématique-de-propagation-dune-épidémie'.

[8] M. A. Aziz-Alaoui *et al.*, 'Etude de Quelques Modèles Epidémiologiques de Métapopulations : Application au Paludisme et à la Tuberculose'.

[9] W. Cota, D. Soriano-Paños, A. Arenas, S. C. Ferreira, and J. Gómez-Gardeñes, 'Infectious disease dynamics in metapopulations with heterogeneous transmission and recurrent mobility', *New J. Phys.*, vol. 23, no. 7, p. 073019, July 2021, doi: 10.1088/1367-2630/ac0c99.

[10] J. Arino, 'Diseases in Metapopulations', in *Series in Contemporary Applied Mathematics*, vol. 11, CO-PUBLISHED WITH HIGHER EDUCATION PRESS, 2009, pp. 64–122. doi: 10.1142/9789814261265_0003.

[11] M. J. Keeling, O. N. Bjørnstad, and B. T. Grenfell, '17. METAPOPULATION DYNAMICS OF'.

[12] M. M. Herman, P. G. Patience, N. Marcial, M. K. Lea, K. M. Peter, and C. M. Benjamin, 'Analyzing and Controlling COVID-19 Using SageMath Toolbox: A case Study in the D.R. Congo', vol. 9, no. 4.

[13] J. Arino, 'Quelques notions d'épidémiologie mathématique'.

[14] A. Apolloni, C. Poletto, J. J. Ramasco, P. Jensen, and V. Colizza, 'Metapopulation epidemic models with heterogeneous mixing and travel behaviour', *Theor. Biol. Med. Model.*, vol. 11, no. 1, p. 3, Dec. 2014, doi: 10.1186/1742-4682-11-3.

[15] S. Léger, 'PROTOCOLE DE TRAITEMENT DE MONKEYPOX SIMPLE ET COMPLIQUE'.

[16] 'Mpox_USPPI-2024'.

[17] Z. Shuai and P. Van Den Driessche, 'Global Stability of Infectious Disease Models Using Lyapunov Functions', *SIAM J. Appl. Math.*, vol. 73, no. 4, pp. 1513–1532, Jan. 2013, doi: 10.1137/120876642.

[18] D. Bichara, 'Étude de modèles épidémiologiques: Stabilité, observation et estimation de paramètres'.

[19] E. J. Dansu and H. Seno, 'A model for epidemic dynamics in a community with visitor subpopulation', *J. Theor. Biol.*, vol. 478, pp. 115–127, Oct. 2019, doi: 10.1016/j.jtbi.2019.06.020.

[20] S. Wang, B. Haegeman, and M. Loreau, 'Dispersal and metapopulation stability', *PeerJ*, vol. 3, p. e1295, Oct. 2015, doi: 10.7717/peerj.1295.

[21] M. Maliyoni, H. D. Gaff, K. S. Govinder, and F. Chirove, 'Multipatch stochastic epidemic model for the dynamics of a tick-borne disease', *Front. Appl. Math. Stat.*, vol. 9, p. 1122410, June 2023, doi: 10.3389/fams.2023.1122410.